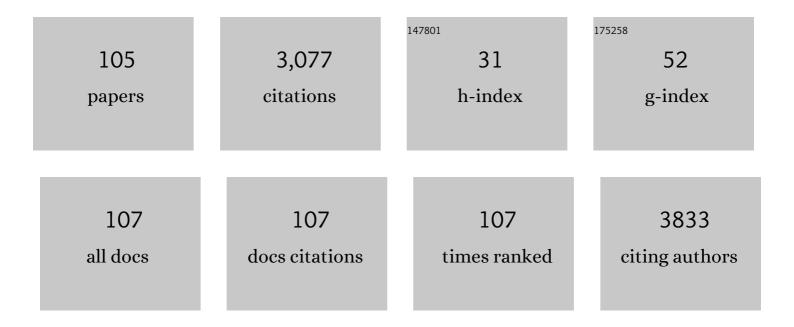
List of Publications by Year in descending order

Source: https://exaly.com/author-pdf/9497249/publications.pdf Version: 2024-02-01



#	Article	IF	CITATIONS
1	Quantitatively Discriminating Alcohol Molecules by Thermally Modulating NiOâ€Based Sensor Arrays. Advanced Materials Technologies, 2022, 7, 2100762.	5.8	6
2	Micro- and Nanopore Technologies for Single-Cell Analysis. , 2022, , 343-373.		0
3	Mechanistic Approach for Long-Term Stability of a Polyethylene Glycol–Carbon Black Nanocomposite Sensor. ACS Sensors, 2022, 7, 151-158.	7.8	3
4	Impact of Lateral SnO <sub>2</sub> Nanofilm Channel Geometry on a 1024 Crossbar Chemical Sensor Array. ACS Sensors, 2022, 7, 460-468.	7.8	6
5	Water-Selective Nanostructured Dehumidifiers for Molecular Sensing Spaces. ACS Sensors, 2022, 7, 534-544.	7.8	3
6	Core-shell Metal Oxide Nanowire Array to Analyze Adsorption Behaviors of Volatile Molecules. Chemistry Letters, 2022, 51, 424-427.	1.3	1
7	Moderate molecular recognitions on ZnO <i>m</i> -plane and their selective capture/release of bio-related phosphoric acids. Nanoscale Advances, 2022, 4, 1649-1658.	4.6	1
8	Edge-Topological Regulation for <i>in Situ</i> Fabrication of Bridging Nanosensors. Nano Letters, 2022, 22, 2569-2577.	9.1	3
9	Surface Dissociation Effect on Phosphonic Acid Self-Assembled Monolayer Formation on ZnO Nanowires. ACS Omega, 2022, 7, 1462-1467.	3.5	3
10	Nanocellulose Paper Semiconductor with a 3D Network Structure and Its Nano–Micro–Macro Trans-Scale Design. ACS Nano, 2022, 16, 8630-8640.	14.6	21
11	Breath odor-based individual authentication by an artificial olfactory sensor system and machine learning. Chemical Communications, 2022, 58, 6377-6380.	4.1	9
12	The impact of surface Cu <sup>2+</sup> of ZnO/(Cu <sub>1â^'x</sub> Zn <sub>x</sub> )O heterostructured nanowires on the adsorption and chemical transformation of carbonyl compounds. Chemical Science, 2021, 12, 5073-5081.	7.4	5
13	Nanowire-based sensor electronics for chemical and biological applications. Analyst, The, 2021, 146, 6684-6725.	3.5	16
14	Enhancement of pH Tolerance in Conductive Al-Doped ZnO Nanofilms via Sequential Annealing. ACS Applied Electronic Materials, 2021, 3, 955-962.	4.3	4
15	Metal–Oxide Nanowire Molecular Sensors and Their Promises. Chemosensors, 2021, 9, 41.	3.6	30
16	Rational Strategy for Space-Confined Seeded Growth of ZnO Nanowires in Meter-Long Microtubes. ACS Applied Materials & Interfaces, 2021, 13, 16812-16819.	8.0	4
17	Maximizing Conversion of Surface Click Reactions for Versatile Molecular Modification on Metal Oxide Nanowires. Langmuir, 2021, 37, 5172-5179.	3.5	3
18	Fabrication of a Robust In2O3 Nanolines FET Device as a Biosensor Platform. Micromachines, 2021, 12, 642.	2.9	8

#	Article	IF	CITATIONS
19	Robust and Electrically Conductive ZnO Thin Films and Nanostructures: Their Applications in Thermally and Chemically Harsh Environments. ACS Applied Electronic Materials, 2021, 3, 2925-2940.	4.3	5
20	Oxide Nanowire Microfluidic Devices for Capturing Single-stranded DNAs. Analytical Sciences, 2021, 37, 1139-1145.	1.6	7
21	Molecular profiling of extracellular vesicles via charge-based capture using oxide nanowire microfluidics. Biosensors and Bioelectronics, 2021, 194, 113589.	10.1	15
22	A thermally robust and strongly oxidizing surface of WO <sub>3</sub> hydrate nanowires for electrical aldehyde sensing with long-term stability. Journal of Materials Chemistry A, 2021, 9, 5815-5824.	10.3	11
23	ZnO/SiO <sub>2</sub> core/shell nanowires for capturing CpG rich single-stranded DNAs. Analytical Methods, 2021, 13, 337-344.	2.7	4
24	Selfâ€Antiâ€Stacking 2D Metal Phosphide Loopâ€Sheet Heterostructures by Edgeâ€Topological Regulation for Highly Efficient Water Oxidation. Small, 2021, 17, e2006860.	10.0	16
25	Image Processing and Machine Learning for Automated Identification of Chemo-/Biomarkers in Chromatography–Mass Spectrometry. Analytical Chemistry, 2021, 93, 14708-14715.	6.5	9
26	Discriminating BTX Molecules by the Nonselective Metal Oxide Sensor-Based Smart Sensing System. ACS Sensors, 2021, 6, 4167-4175.	7.8	19
27	Synthesis of Monodispersedly Sized ZnO Nanowires from Randomly Sized Seeds. Nano Letters, 2020, 20, 599-605.	9.1	40
28	Identification of Genetic Variants via Bacterial Respiration Gas Analysis. Frontiers in Microbiology, 2020, 11, 581571.	3.5	0
29	Oxygen-Induced Reversible Sn-Dopant Deactivation between Indium Tin Oxide and Single-Crystalline Oxide Nanowire Leading to Interfacial Switching. ACS Applied Materials & Interfaces, 2020, 12, 52929-52936.	8.0	6
30	Artificial visual systems enabled by quasi–two-dimensional electron gases in oxide superlattice nanowires. Science Advances, 2020, 6, .	10.3	51
31	Facile Synthesis of Zinc Titanate Nanotubes via Reaction-byproduct Etching. Chemistry Letters, 2020, 49, 1220-1223.	1.3	0
32	Face-selective tungstate ions drive zinc oxide nanowire growth direction and dopant incorporation. Communications Materials, 2020, 1, .	6.9	12
33	Ammonia-Induced Seed Layer Transformations in a Hydrothermal Growth Process of Zinc Oxide Nanowires. Journal of Physical Chemistry C, 2020, 124, 20563-20568.	3.1	18
34	Perovskite Core–Shell Nanowire Transistors: Interfacial Transfer Doping and Surface Passivation. ACS Nano, 2020, 14, 12749-12760.	14.6	34
35	Phosphonic Acid Modified ZnO Nanowire Sensors: Directing Reaction Pathway of Volatile Carbonyl Compounds. ACS Applied Materials & Interfaces, 2020, 12, 44265-44272.	8.0	19
36	Unusual Sequential Annealing Effect in Achieving High Thermal Stability of Conductive Al-Doped ZnO Nanofilms. ACS Applied Electronic Materials, 2020, 2, 2064-2070.	4.3	10

#	Article	IF	CITATIONS
37	Monovalent sulfur oxoanions enable millimeter-long single-crystalline <i>h</i> -WO <sub>3</sub> nanowire synthesis. Nanoscale, 2020, 12, 9058-9066.	5.6	7
38	Mechanical Rupture-Based Antibacterial and Cell-Compatible ZnO/SiO2 Nanowire Structures Formed by Bottom-Up Approaches. Micromachines, 2020, 11, 610.	2.9	17
39	Face-Selective Crystal Growth of Hydrothermal Tungsten Oxide Nanowires for Sensing Volatile Molecules. ACS Applied Nano Materials, 2020, 3, 10252-10260.	5.0	8
40	Photolithographically Constructed Single ZnO Nanowire Device and Its Ultraviolet Photoresponse. Analytical Sciences, 2020, 36, 1125-1129.	1.6	7
41	Micro- and Nanopore Technologies for Single-Cell Analysis. , 2020, , 1-31.		0
42	Substantial Narrowing on the Width of "Concentration Window―of Hydrothermal ZnO Nanowires via Ammonia Addition. Scientific Reports, 2019, 9, 14160.	3.3	33
43	Peptide Screening from a Phage Display Library for Benzaldehyde Recognition. Chemistry Letters, 2019, 48, 978-981.	1.3	12
44	Redox-Inactive CO <sub>2</sub> Determines Atmospheric Stability of Electrical Properties of ZnO Nanowire Devices through a Room-Temperature Surface Reaction. ACS Applied Materials & Interfaces, 2019, 11, 40260-40266.	8.0	12
45	Growth Kinetics and Magnetic Property of Single-Crystal Fe Nanowires Grown via Vapor–Solid Mechanism Using Chemically Synthesized FeO Nanoparticle Catalysts. Crystal Growth and Design, 2019, 19, 7257-7263.	3.0	1
46	Controlling Bi-Provoked Nanostructure Formation in GaAs/GaAsBi Core–Shell Nanowires. Nano Letters, 2019, 19, 8510-8518.	9.1	11
47	Water–Organic Cosolvent Effect on Nucleation of Solution-Synthesized ZnO Nanowires. ACS Omega, 2019, 4, 8299-8304.	3.5	10
48	Discrimination of VOCs molecules via extracting concealed features from a temperature-modulated p-type NiO sensor. Sensors and Actuators B: Chemical, 2019, 293, 342-349.	7.8	60
49	Rational Method of Monitoring Molecular Transformations on Metal-Oxide Nanowire Surfaces. Nano Letters, 2019, 19, 2443-2449.	9.1	21
50	Unusual Oxygen Partial Pressure Dependence of Electrical Transport of Single-Crystalline Metal Oxide Nanowires Grown by the Vapor–Liquid–Solid Process. Nano Letters, 2019, 19, 1675-1681.	9.1	5
51	Paper-Based Disposable Molecular Sensor Constructed from Oxide Nanowires, Cellulose Nanofibers, and Pencil-Drawn Electrodes. ACS Applied Materials & Interfaces, 2019, 11, 15044-15050.	8.0	54
52	Engineering Nanowire-Mediated Cell Lysis for Microbial Cell Identification. ACS Nano, 2019, 13, 2262-2273.	14.6	17
53	Low-Power and ppm-Level Multimolecule Detection by Integration of Self-Heated Metal Nanosheet Sensors. IEEE Transactions on Electron Devices, 2019, 66, 5393-5398.	3.0	15
54	A real-time simultaneous measurement on a microfluidic device for individual bacteria discrimination. Sensors and Actuators B: Chemical, 2018, 260, 746-752.	7.8	17

#	Article	IF	CITATIONS
55	Robust Ionic Current Sensor for Bacterial Cell Size Detection. ACS Sensors, 2018, 3, 574-579.	7.8	13
56	Effect of Channel Geometry on Ionic Current Signal of a Bridge Circuit Based Microfluidic Channel. Chemistry Letters, 2018, 47, 350-353.	1.3	5
57	PM <sub>2.5</sub> Particle Detection in a Microfluidic Device by Using Ionic Current Sensing. Analytical Sciences, 2018, 34, 1347-1349.	1.6	6
58	Biomolecular recognition on nanowire surfaces modified by the self-assembled monolayer. Lab on A Chip, 2018, 18, 3225-3229.	6.0	15
59	Integrated molecule recognition sensor electronics using nanostructured metal oxides on silicon. , 2018, , .		0
60	Thermal conductivity of Si nanowires with δ-modulated dopant distribution by self-heated 3ω method and its length dependence. Journal of Applied Physics, 2018, 124, 065105.	2.5	8
61	A millisecond micro-RNA separation technique by a hybrid structure of nanopillars and nanoslits. Scientific Reports, 2017, 7, 43877.	3.3	13
62	Long-Term Stability of Oxide Nanowire Sensors via Heavily Doped Oxide Contact. ACS Sensors, 2017, 2, 1854-1859.	7.8	24
63	Substantial Expansion of Detectable Size Range in Ionic Current Sensing through Pores by Using a Microfluidic Bridge Circuit. Journal of the American Chemical Society, 2017, 139, 14137-14142.	13.7	39
64	Unveiling massive numbers of cancer-related urinary-microRNA candidates via nanowires. Science Advances, 2017, 3, e1701133.	10.3	170
65	True Vapor–Liquid–Solid Process Suppresses Unintentional Carrier Doping of Single Crystalline Metal Oxide Nanowires. Nano Letters, 2017, 17, 4698-4705.	9.1	20
66	Discriminating single-bacterial shape using low-aspect-ratio pores. Scientific Reports, 2017, 7, 17371.	3.3	58
67	Effect of DNA Methylation on the Velocity of DNA Translocation through a Nanochannel. Analytical Sciences, 2017, 33, 727-730.	1.6	1
68	Nanostructures Integrated with a Nanochannel for Slowing Down DNA Translocation Velocity for Nanopore Sequencing. Analytical Sciences, 2017, 33, 735-738.	1.6	1
69	Fabrication of Single Crystalline Metal Oxide Nanowires Based on Spatial Selectivity of Molecules. Hyomen Kagaku, 2017, 38, 351-356.	0.0	0
70	Nanoscale Thermal Management of Single SnO <sub>2</sub> Nanowire: pico-Joule Energy Consumed Molecule Sensor. ACS Sensors, 2016, 1, 997-1002.	7.8	56
71	Rational Concept for Reducing Growth Temperature in Vapor–Liquid–Solid Process of Metal Oxide Nanowires. Nano Letters, 2016, 16, 7495-7502.	9.1	33
72	Nanostructuration of PEDOT in Porous Coordination Polymers for Tunable Porosity and Conductivity. Journal of the American Chemical Society, 2016, 138, 10088-10091.	13.7	193

#	Article	IF	CITATIONS
73	All-nanocellulose nonvolatile resistive memory. NPG Asia Materials, 2016, 8, e310-e310.	7.9	64
74	Tailoring Nucleation at Two Interfaces Enables Single Crystalline NiO Nanowires via Vapor–Liquid–Solid Route. ACS Applied Materials & Interfaces, 2016, 8, 27892-27899.	8.0	6
75	Identifying DNA methylation in a nanochannel. Science and Technology of Advanced Materials, 2016, 17, 644-649.	6.1	11
76	Three-dimensional Nanowire Structures for Ultra-Fast Separation of DNA, Protein and RNA Molecules. Scientific Reports, 2015, 5, 10584.	3.3	39
77	A oxide nanowire for probing nanoscale memristive switching. , 2015, , .		0
78	Rational Concept for Designing Vapor–Liquid–Solid Growth of Single Crystalline Metal Oxide Nanowires. Nano Letters, 2015, 15, 6406-6412.	9.1	46
79	A flux induced crystal phase transition in the vapor–liquid–solid growth of indium-tin oxide nanowires. Nanoscale, 2014, 6, 7033.	5.6	20
80	Modulation of Thermoelectric Power Factor via Radial Dopant Inhomogeneity in B-Doped Si Nanowires. Journal of the American Chemical Society, 2014, 136, 14100-14106.	13.7	16
81	Ultrafast and Wide Range Analysis of DNA Molecules Using Rigid Network Structure of Solid Nanowires. Scientific Reports, 2014, 4, 5252.	3.3	54
82	Cellulose Nanofiber Paper as an Ultra Flexible Nonvolatile Memory. Scientific Reports, 2014, 4, 5532.	3.3	122
83	Crystal-Plane Dependence of Critical Concentration for Nucleation on Hydrothermal ZnO Nanowires. Journal of Physical Chemistry C, 2013, 117, 1197-1203.	3.1	67
84	Impact of Preferential Indium Nucleation on Electrical Conductivity of Vapor–Liquid–Solid Grown Indium–Tin Oxide Nanowires. Journal of the American Chemical Society, 2013, 135, 7033-7038.	13.7	44
85	Advanced Photoassisted Atomic Switches Produced Using ITO Nanowire Electrodes and Molten Photoconductive Organic Semiconductors. Advanced Materials, 2013, 25, 5893-5897.	21.0	11
86	DNA Manipulation and Separation in Sublithographic-Scale Nanowire Array. ACS Nano, 2013, 7, 3029-3035.	14.6	61
87	Scaling Effect on Unipolar and Bipolar Resistive Switching of Metal Oxides. Scientific Reports, 2013, 3, 1657.	3.3	87
88	Switching Properties of Titanium Dioxide Nanowire Memristor. Japanese Journal of Applied Physics, 2012, 51, 11PE09.	1.5	10
89	Dual Defects of Cation and Anion in Memristive Nonvolatile Memory of Metal Oxides. Journal of the American Chemical Society, 2012, 134, 2535-2538.	13.7	44
90	Fundamental Strategy for Creating VLS Grown TiO <sub>2</sub> Single Crystalline Nanowires. Journal of Physical Chemistry C, 2012, 116, 24367-24372.	3.1	28

#	Article	IF	CITATIONS
91	Prominent Thermodynamical Interaction with Surroundings on Nanoscale Memristive Switching of Metal Oxides. Nano Letters, 2012, 12, 5684-5690.	9.1	40
92	Intrinsic Mechanisms of Memristive Switching. Nano Letters, 2011, 11, 2114-2118.	9.1	110
93	Study on transport pathway in oxide nanowire growth by using spacing-controlled regular array. Applied Physics Letters, 2011, 99, 193105.	3.3	20
94	Essential role of catalyst in vapor-liquid-solid growth of compounds. Physical Review E, 2011, 83, 061606.	2.1	20
95	Impurity induced periodic mesostructures in Sb-doped SnO2 nanowires. Journal of Crystal Growth, 2010, 312, 3251-3256.	1.5	10
96	Interfacial effect on metal/oxide nanowire junctions. Applied Physics Letters, 2010, 96, 073110.	3.3	29
97	Numerical study on the difference in mechanism between vapor-solid and vapor-liquid-solid solid solid solid solid fication processes. Physical Review E, 2010, 82, 011605.	2.1	11
98	Resistive-Switching Memory Effects of NiO Nanowire/Metal Junctions. Journal of the American Chemical Society, 2010, 132, 6634-6635.	13.7	125
99	Role of surrounding oxygen on oxide nanowire growth. Applied Physics Letters, 2010, 97, 073114.	3.3	40
100	Resistive Switching Multistate Nonvolatile Memory Effects in a Single Cobalt Oxide Nanowire. Nano Letters, 2010, 10, 1359-1363.	9.1	239
101	Crucial role of doping dynamics on transport properties of Sb-doped SnO2 nanowires. Applied Physics Letters, 2009, 95, 053105.	3.3	39
102	Nonvolatile Bipolar Resistive Memory Switching in Single Crystalline NiO Heterostructured Nanowires. Journal of the American Chemical Society, 2009, 131, 3434-3435.	13.7	147
103	Enhancement of Oxide VLS Growth by Carbon on Substrate Surface. Journal of Physical Chemistry C, 2008, 112, 18923-18926.	3.1	41
104	Mechanism and control of sidewall growth and catalyst diffusion on oxide nanowire vapor-liquid-solid growth. Applied Physics Letters, 2008, 93, .	3.3	56
105	Mechanism of catalyst diffusion on magnesium oxide nanowire growth. Applied Physics Letters, 2007, 91, .	3.3	54